



## **Search for a long-lived scalar at Belle II: plots for approval for Long-lived particles at Belle II Workshop**

The Belle II Collaboration

This note presents studies in the context of the search for a long-lived scalar at Belle II using simulated signal and background samples. The search focusses on reconstructing a neutral long-lived particle from two charged tracks forming a displaced vertex. The simulated samples used for the studies and the currently used signal selection variables are described. Presented are plots to be approved that show these selection variables for simulated background and signal samples, as well as the simulated displaced vertex reconstruction performance at Belle II.

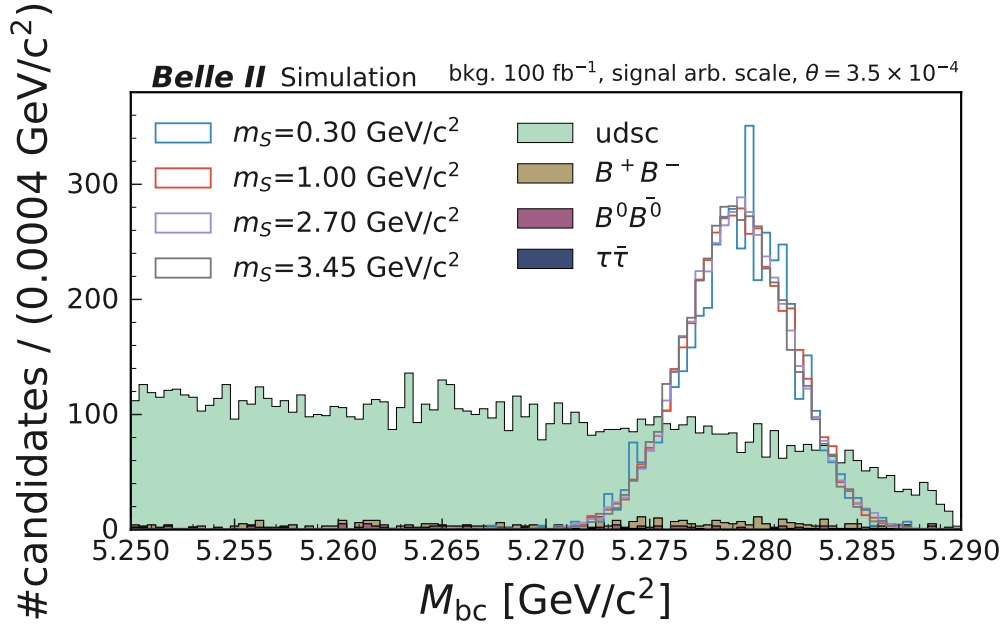


FIG. 1: The  $M_{bc}$  distribution for the background samples, and signal models at different masses and the same mixing angle. The signal samples show the typical peaking shape around the  $B$  mass, while backgrounds from non- $B$  samples feature a slowly falling distribution with a quick drop to the kinematic endpoint.

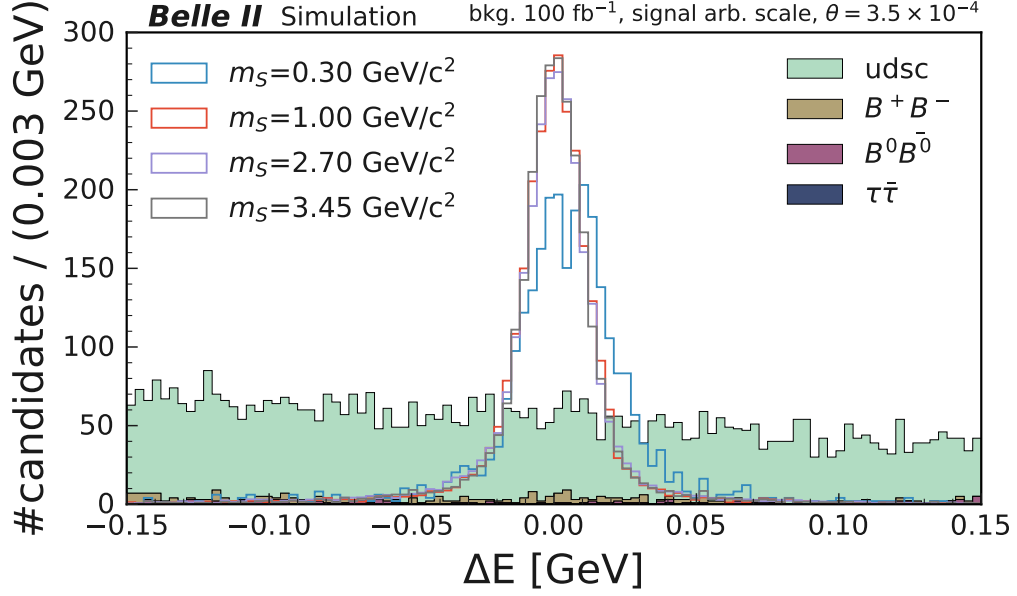


FIG. 2: The  $\Delta E$  distribution for the background samples, and signal models at different masses and the same mixing angle. The signal samples show the typical peaking shape around zero, while backgrounds from non- $B$  samples show a slowly falling behaviour from negative to positive  $\Delta E$  values. The low mass sample has a considerably larger lifetime at the same mixing angle compared to the larger mass samples. The  $\Delta E$  variable shows a larger sensitivity to effects of the larger lifetime for small scalar masses, resulting in the slight shift in the blue distribution.

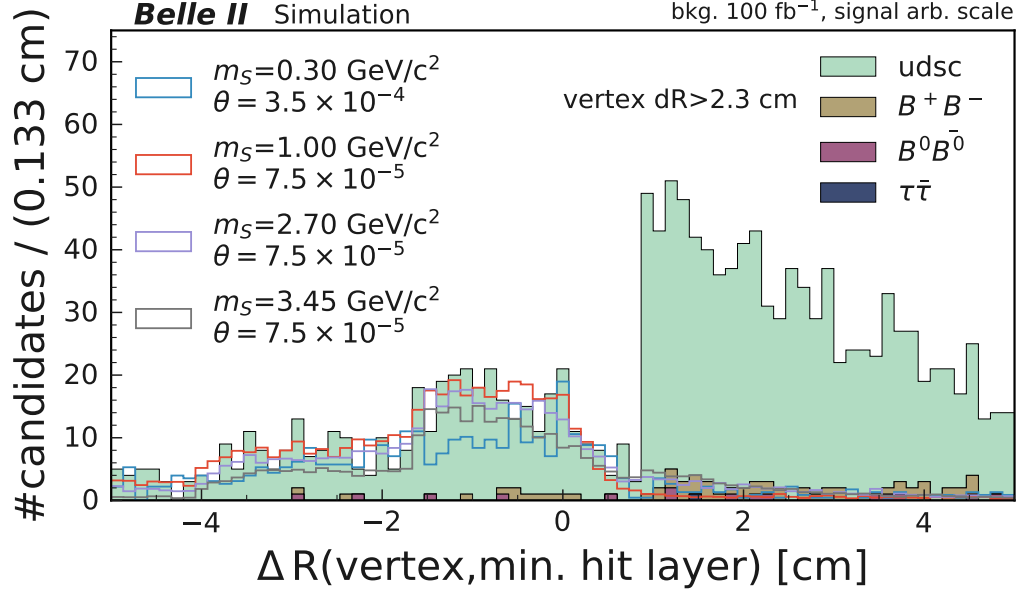


FIG. 3: The  $\Delta dR(\text{vertex, min. layer})$  distribution for the background samples, and for signal samples at different masses and mixing angles. The lower mixing angles are chosen to enrich the samples with larger flight distances due to the longer scalar lifetimes. The analysis variable is particularly useful for longer lifetimes to reject fake  $V0$ 's when the vertex is further away from the IP and the hypothetical long-lived particle has passed tracking layers. An additional cut on the minimum displacement is added to ensure that the vertex is past the first tracking layer to showcase the variable. The signal-like background is mostly due to remaining SM  $V0$ 's such as  $K_S^0$  and  $\Lambda^0$ . The sharp edge around 0.7 cm is produced by random track combinations with a vertex  $dR$  starting at 2.3 cm where at least one of the tracks features a hit in the detector layer at 1.4 cm.

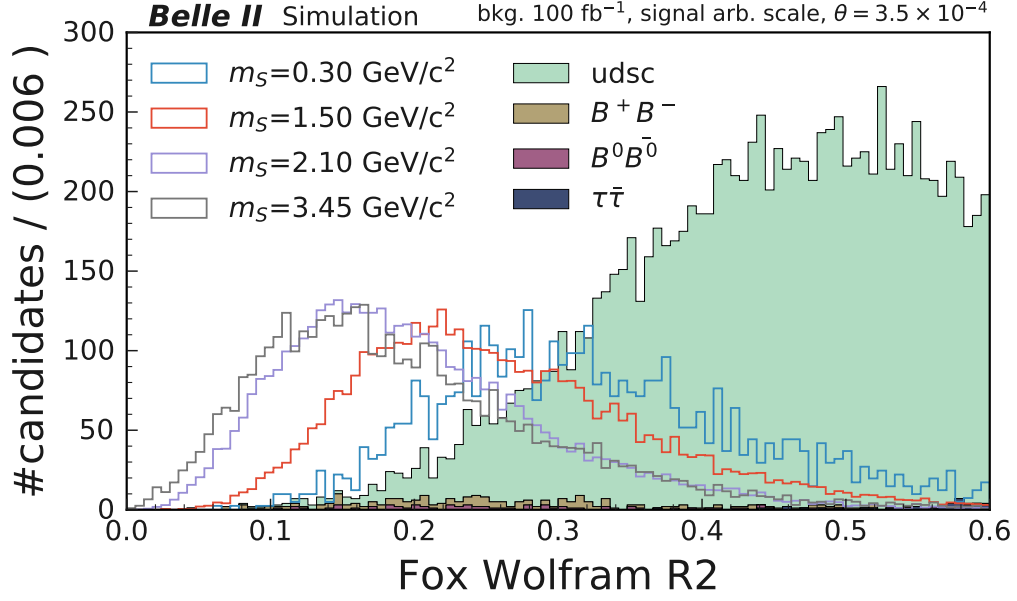


FIG. 4: The Fox Wolfram R2 distribution for the background samples, and for signal samples at different masses and the same mixing angle. The signal distributions tend to lower values as expected for  $B\bar{B}$  events. The non- $B$  background samples feature a distribution centered at larger values. The scalar is less boosted for large scalar masses, resulting in a more spherical distribution of the momenta. This improves the separation in R2 between continuum and signal for increasing scalar mass.

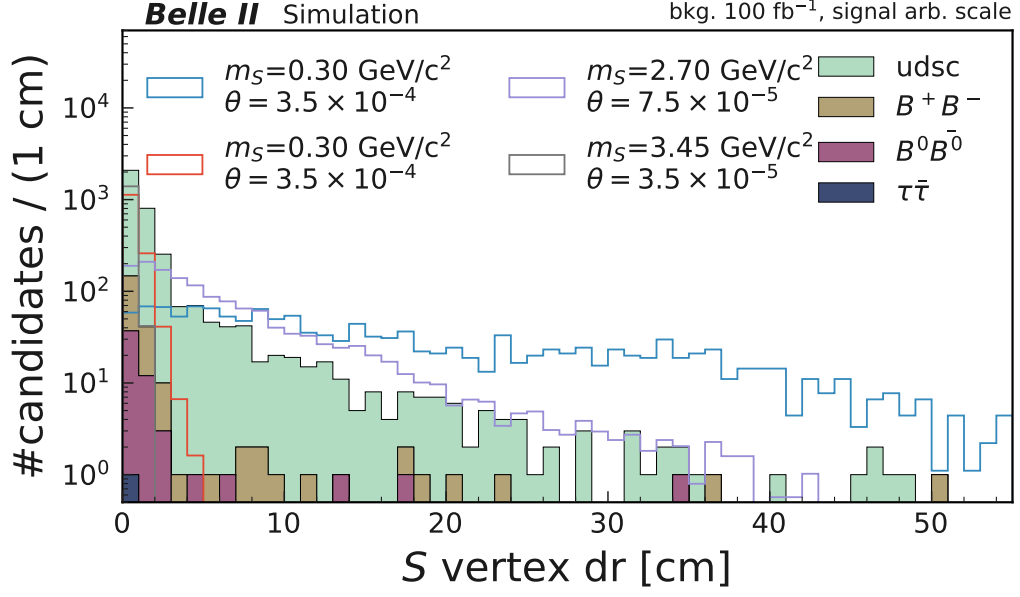


FIG. 5: The scalar  $dR$  distribution for the background samples, and for signal samples at different masses and mixing angles. All analysis cuts as described above are implemented. The lifetime of the scalar is dependent on the mixing angle but also its mass. The remaining background sources are mainly at low displacements. To test signal models with a large lifetime, a tighter (larger) minimum displacement cut will be worthwhile.

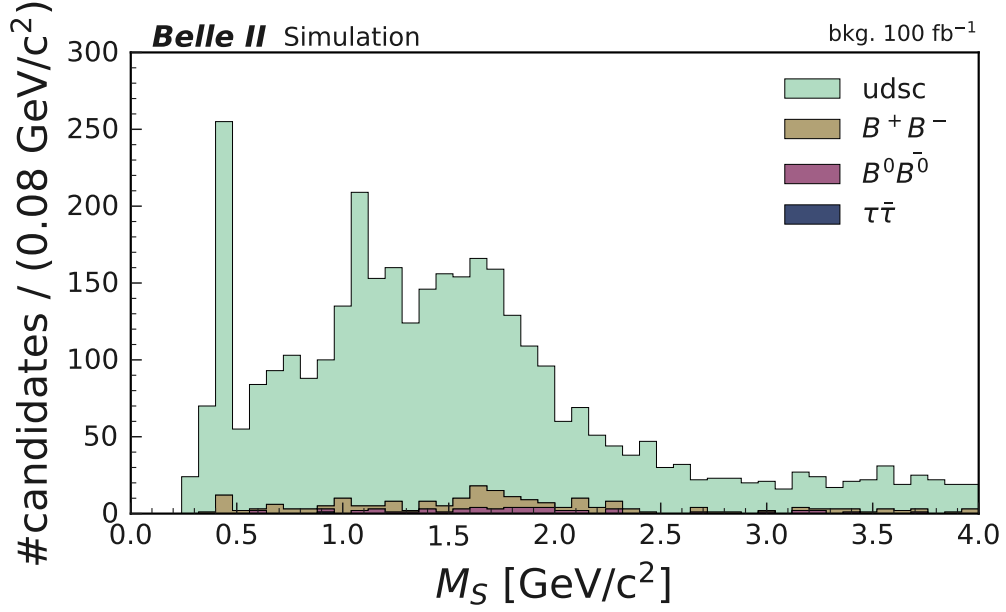


FIG. 6: The  $m_S$  distribution for the background samples. The signal is not shown in this range as the signal mass resolution is small enough for nearly the complete distributions to lie each within one bin. Signal and background expectations will be compared in bins of this distributions with a size proportional to the mass resolution. The background distribution feature remaining contamination from true  $K_S^0$  in the  $\mu^+\mu^-$  channel (slightly below the  $K_S^0$  mass) and in the  $K^+ K^-$  channel (around 1  $\text{GeV}/c^2$ ).

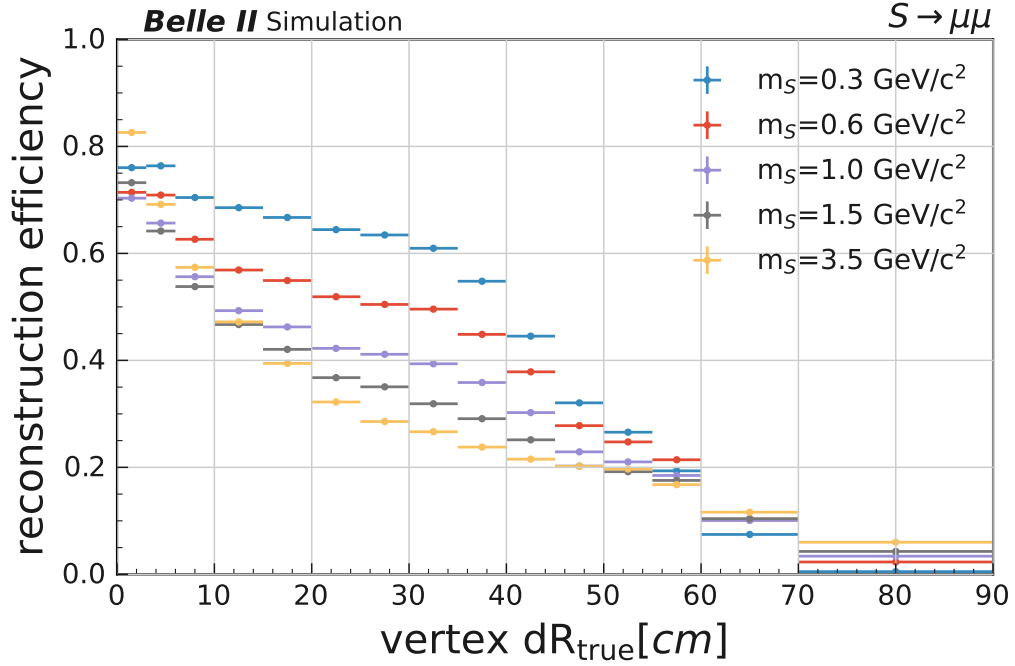


FIG. 7: The reconstruction efficiency for  $S \rightarrow \mu^+ \mu^-$  in bins of the true vertex displacement in  $R$  for different scalar masses. The efficiency is determined using the flat lifetime samples described above, and by truth-matching the reconstructed candidates. An uncertainty is calculated and plotted but very small due to the large statistics in the sample. The reconstruction efficiency is large at low displacements but drops considerably after a few cm. At large masses, the opening angle between tracks is larger. This leads to more tracks being outside the detector acceptance, and tracks that are less pointing towards the interaction point. This reduces the reconstruction efficiency for larger masses.

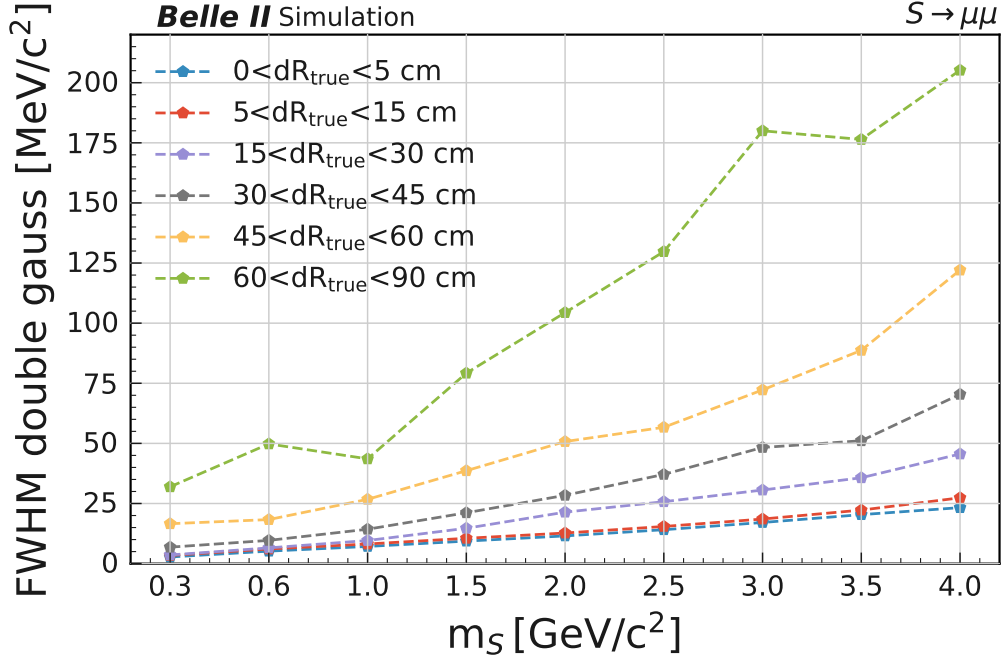


FIG. 8: The scalar mass resolution when reconstructing  $S \rightarrow \mu^+\mu^-$  for different masses and in different bins of true vertex displacement. The reconstructed mass distribution is fitted with a double gaussian and the full width at half maximum is calculated as a figure of merit for the resolution. The mass resolution is very good across different masses and for most of the vertex displacement regions. At very large displacements the resolutions worsens because both, the initial track momentum and vertex position which updates the momenta become difficult to determine with the small number of track hits. Errorbars are not shown, the dashed lines between the points are drawn to guide the eye.

## 1. REFERENCES